

Post– versus pre–resonance characteristics of axially excited chiral sculptured thin films

Akhlesh Lakhtakia¹ and Jason T. Moyer

CATMAS — Computational & Theoretical Materials Sciences Group

Department of Engineering Science & Mechanics

Pennsylvania State University, University Park, PA 16802–6812, USA

Abstract. Axially excited chiral sculptured thin films (STFs) are shown to exhibit the circular Bragg phenomenon in the pre–resonant (long–wavelength) regime but not in some parts of the post–resonant (short–wavelength) regime. Chiral STFs act as very good polarization–independent reflectors in the vicinity of material resonances in the latter regime.

Keywords: Circular Bragg phenomenon; Chiral sculptured thin films; Lorentz model; Resonance

1 Introduction

The chief optical signature of a chiral sculptured thin film (STF) is the circular Bragg phenomenon it displays on axial excitation [1, 2]. A chiral STF is modeled as a unidirectionally nonhomogeneous dielectric continuum with a permittivity dyadic that varies periodically along, say, the z axis in a helicoidal fashion. Let a circularly polarized plane wave with free–space wavelength λ_0 axially excite a chiral STF of finite thickness. Provided that the film thickness is sufficiently large and λ_0 lies within the so–called Bragg regime, the reflectance is much higher if the handedness of the incident plane wave matches its structural handedness than if otherwise. Indeed, light of one circular polarization — coincident with the structural handedness of the chiral STF — effectively encounters a grating in the Bragg regime, while light of the opposite circular polarization state does not [3, 4]. The described phenomenon has been theoretically

¹Tel: +1-814-863-4319, Fax: +1-814-863-7967, e-mail: AXL4@psu.edu

established for chiral STF half-spaces as well [5, 6].

Explicit in the theoretical research [1, 7], and implicit in the experimental research [8, 9, 10], on STFs thus far is the supposition that the real parts of all cartesian components of the permittivity dyadic of a chiral STF are positive real. Viewed through the lens of the Lorentz one-resonance model [11], consideration has been essentially restricted to the pre-resonant (or the long-wavelength) regime. The response of a chiral STF in the post-resonant (or the short-wavelength) regime is simply unknown, which lacuna motivated the work presented here.

Accordingly, in this communication, we present the reflection characteristics of an axially excited chiral STF half-space, and compare the pre- and the post-resonant signatures. A note on notation: Vectors are underlined, dyadics are double-underlined; while an $\exp(-i\omega t)$ time-dependence is implicit, with ω as the angular frequency.

2 Theoretical Preliminaries

The dielectric properties of the chiral STF are delineated by the nonhomogeneous permittivity dyadic [1]

$$\underline{\underline{\epsilon}}(\underline{x}) = \epsilon_0 \underline{\underline{S}}_z(z, h) \cdot \underline{\underline{S}}_y(\chi) \cdot \underline{\underline{\epsilon}}_{ref}^o \cdot \underline{\underline{S}}_y^{-1}(\chi) \cdot \underline{\underline{S}}_z^{-1}(z, h); \quad z \geq 0, \quad (1)$$

where

$$\underline{\underline{\epsilon}}_{ref}^o = \epsilon_a \underline{\underline{u}}_z \underline{\underline{u}}_z + \epsilon_b \underline{\underline{u}}_x \underline{\underline{u}}_x + \epsilon_c \underline{\underline{u}}_y \underline{\underline{u}}_y. \quad (2)$$

Here and hereafter, ϵ_0 and μ_0 are the permittivity and the permeability of free space (i.e., vacuum), respectively; $k_0 = 2\pi/\lambda_0 = \omega \sqrt{\mu_0 \epsilon_0}$ is the wavelength in free space; $\underline{\underline{u}}_x$, $\underline{\underline{u}}_y$ and $\underline{\underline{u}}_z$ denote the unit cartesian vectors; while $\epsilon_{a,b,c}$ are complex-valued functions of ω . The rotation dyadic

$$\begin{aligned} \underline{\underline{S}}_z(z, h) &= \underline{\underline{u}}_z \underline{\underline{u}}_z + \left(\underline{\underline{u}}_x \underline{\underline{u}}_x + \underline{\underline{u}}_y \underline{\underline{u}}_y \right) \cos \frac{\pi z}{\Omega} \\ &\quad + h \left(\underline{\underline{u}}_y \underline{\underline{u}}_x - \underline{\underline{u}}_x \underline{\underline{u}}_y \right) \sin \frac{\pi z}{\Omega} \end{aligned} \quad (3)$$

captures the helicoidal periodicity of the STF, with 2Ω being the structural period. The integer $h = 1$ for a structurally right-handed chiral STF; and $h = -1$ for structural left-handedness.

The tilt dyadic

$$\underline{\underline{S}}_y(\chi) = \underline{u}_y \underline{u}_y + (\underline{u}_x \underline{u}_x + \underline{u}_z \underline{u}_z) \cos \chi + (\underline{u}_z \underline{u}_x - \underline{u}_x \underline{u}_z) \sin \chi \quad (4)$$

represents the *locally* aciculate microstructure of the chiral STF. In the present context, the most interesting properties of axially excited chiral STFs depend on Ω , ϵ_c and

$$\tilde{\epsilon}_d = \epsilon_a \epsilon_b / (\epsilon_a \cos^2 \chi + \epsilon_b \sin^2 \chi). \quad (5)$$

Suppose an arbitrarily polarized plane wave is normally incident on the chiral STF half-space from the lower half-space $z \leq 0$, which is vacuum. As a result, a plane wave is reflected into the lower half-space. The electric field phasor associated with the two plane waves in the lower half-space is stated as

$$\begin{aligned} \underline{E}(z) &= (a_L \underline{u}_+ + a_R \underline{u}_-) \exp(ik_0 z) \\ &+ (r_L \underline{u}_- + r_R \underline{u}_+) \exp(-ik_0 z); \quad z \leq 0, \end{aligned} \quad (6)$$

and the corresponding magnetic field phasor is then easily determined from the Faraday equation. Here, the complex unit vectors $\underline{u}_\pm = (\underline{u}_x \pm i\underline{u}_y)/\sqrt{2}$; a_L and a_R are the known amplitudes of the left- and the right-circularly polarized components of the incident plane wave; and r_L and r_R are the unknown amplitudes of the reflected planewave components.

Our attention is focussed in this communication on the reflection coefficients entering the 2×2 matrix in the following relation:

$$\begin{bmatrix} r_L \\ r_R \end{bmatrix} = \begin{bmatrix} r_{LL} & r_{LR} \\ r_{RL} & r_{RR} \end{bmatrix} \begin{bmatrix} a_L \\ a_R \end{bmatrix}. \quad (7)$$

These coefficients are doubly subscripted: those with both subscripts identical refer to co-polarized, while those with two different subscripts denote cross-polarized, reflection. These coefficients can be calculated by following the procedure recorded elsewhere [5, 6].

3 Numerical Results and Conclusions

Figure 1 shows plots of the reflectances $R_{LL} = |r_{LL}|^2$, etc. as functions of the parameter Ω/λ_0 when $h = 1$, $\epsilon_c = 3(1 + 0.01i)$ and $\tilde{\epsilon}_d = 3.3(1 + 0.02i)$. These plots hold for the pre-resonant case, because $\text{Re}[\epsilon_c] > 0$ and $\text{Re}[\tilde{\epsilon}_d] > 0$. As predicted, the circular Bragg phenomenon is in evidence as the peak in the plot of R_{RR} at $\Omega/\lambda_0 \approx 0.284$. In contrast, $R_{LL} \simeq 0$ for all values of $\Omega/\lambda_0 \in [0.1, 0.5]$. The cross-polarized reflectances are quite small and also virtually indistinguishable from each other.

In the very short-wavelength portion of the post-resonant regime, $\text{Re}[\epsilon_c] > 0$ and $\text{Re}[\tilde{\epsilon}_d] > 0$ as well. The circular Bragg phenomenon will be exhibited in that portion of the electromagnetic spectrum, just as in the pre-resonant regime, provided that continuum electromagnetic theory remains valid.

However, closer to the material resonances, $\text{Re}[\epsilon_c] < 0$ and $\text{Re}[\tilde{\epsilon}_d] < 0$ in the post-resonant regime. Figure 2 shows plots of the same reflectances as in Figure 1, except that $\epsilon_c = 3(-1 + 0.01i)$ and $\tilde{\epsilon}_d = 3.3(-1 + 0.02i)$. The absence of the circular Bragg phenomenon is conspicuous. Indeed, while both co-polarized reflectances are almost negligible, both cross-polarized reflectances are extremely high. These plots indicate that a post-resonant chiral STF will reflect very well in the vicinity of the material resonances, in the same way that metals do.

The inescapable conclusion is that the circular Bragg phenomenon can be exhibited in the pre-resonance regime but not throughout the post-resonant regime. Thus, soft ultra-violet reflectance spectrums of chiral STFs are unlikely to be interesting for circular-polarization-sensitive reflection applications. Our results also suggest the futility of transmission measurements for characterizing chiral STFs in the long-wavelength portion of the post-resonant regime.

Because of mathematical isomorphism, similar conclusions should hold — other factors aside — for chiral liquid crystals too [12]. Furthermore, as materials with negative real permittivity in the microwave regime have now become artificially possible [13, 14, 15], our conclusions should also apply for synthetic laminar cholesteric materials for duty in that portion of the electromagnetic spectrum.

References

- [1] Venugopal VC, Lakhtakia A: Sculptured thin films: Conception, optical properties, and applications. In: Singh ON, Lakhtakia A (eds): Electromagnetic Fields in Unconventional Materials and Structures. Chap. 5. Wiley, New York, 2000
- [2] Wu Q, Hodgkinson IJ, Lakhtakia A: Circular polarization filters made of chiral sculptured thin films: experimental and simulation results. *Opt. Engg.* **39** (2000) 1863–1868
- [3] McCall MW, Lakhtakia A: Development and assessment of coupled wave theory of axial propagation in thin-film helicoidal bianisotropic media. Part 1: reflectances and transmittances. *J. Modern Opt.* **47** (2000) 973–991
- [4] McCall MW, Lakhtakia A: Development and assessment of coupled wave theory of axial propagation in thin-film helicoidal bi-anisotropic media. Part 2: dichroisms, ellipticity transformation and optical rotation. *J. Modern Opt.* **48** (2001) 143–158
- [5] Lakhtakia A: On percolation and circular Bragg phenomenon in metallic, helicoidally periodic, sculptured thin films. *Microw. Opt. Technol. Lett.* **24** (2000) 239–244 [Two typographical errors need correction: (i) $a_4 \equiv 0$ (but not $a_3 \equiv 0$) when $P_{4z}/|a_4|^2 < 0$; and $r_L - r_R$ should be replaced by $r_L + r_R$ in Eq. (17).]
- [6] Lakhtakia A, McCall MW: Simple expressions for Bragg reflection from axially excited chiral sculptured thin films. *J. Modern Opt.* **00** (2002) 000–000 (accepted in October 2001 for publication)
- [7] Lakhtakia A, Messier R: Sculptured thin films. *OSA Opt. Photon. News* **12** (2001) 26–31 (September issue)
- [8] Sit JC, Broer DJ, Brett MJ: Liquid crystal alignment and switching in porous chiral optical materials. *Adv. Mater.* **12** (2000) 371–373
- [9] Hodgkinson I, Wu Qh: Inorganic chiral optical materials. *Adv. Mater.* **13** (2001) 889–897

- [10] Hodgkinson I, Wu QH, Collett S: Dispersion equations for vacuum-deposited tilted-columnar biaxial media. *Appl. Opt.* **40** (2001) 452–457
- [11] Kittel C: *Introduction to Solid State Physics*, Chap. 13. Wiley Eastern, New Delhi, India 1974
- [12] Chandrasekhar S: *Liquid Crystals*. Cambridge University Press, Cambridge, UK 1992
- [13] Pendry JB, Holden AJ, Robbins DJ, Stewart WJ: Low frequency plasmons in thin-wire structures. *J. Phys.: Condens. Matter* **10** (1998) 4785–4809
- [14] Shelby RA, Smith DR, Schultz S: Experimental verification of a negative index of refraction. *Science* **292** (2001) 77–79
- [15] Lakhtakia A, Slepyan GY, Maksimenko SA: Towards cholesteric absorbers for microwave frequencies. *Int. J. Infrared Millim. Waves* **22** (2001) 999–1007

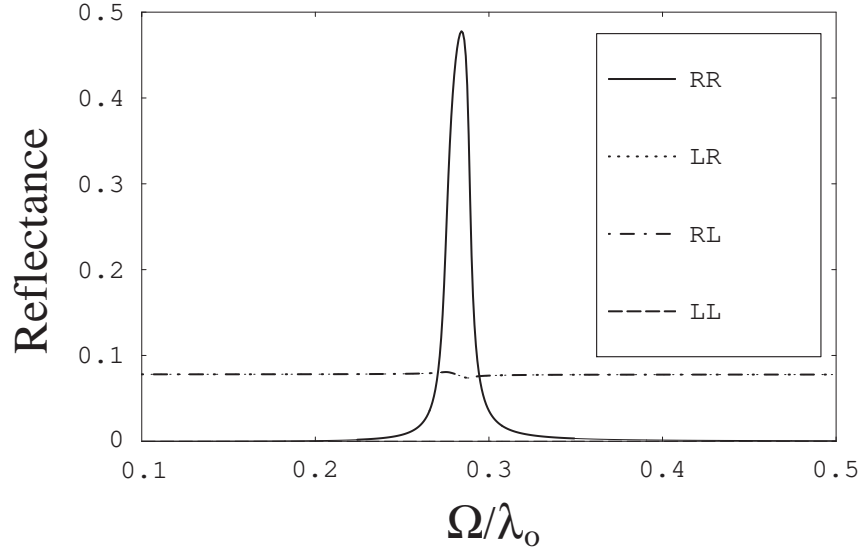


Figure 1: Computed values of the reflectances as functions of Ω/λ_0 , when $h = 1$, $\epsilon_c = 3(1+0.01i)$ and $\tilde{\epsilon}_d = 3.3(1 + 0.02i)$. Note that $R_{RL} \simeq R_{LR}$, as pointed out elsewhere [6]; while $R_{LL} \simeq 0$ cannot be discerned at the scale of the graph.

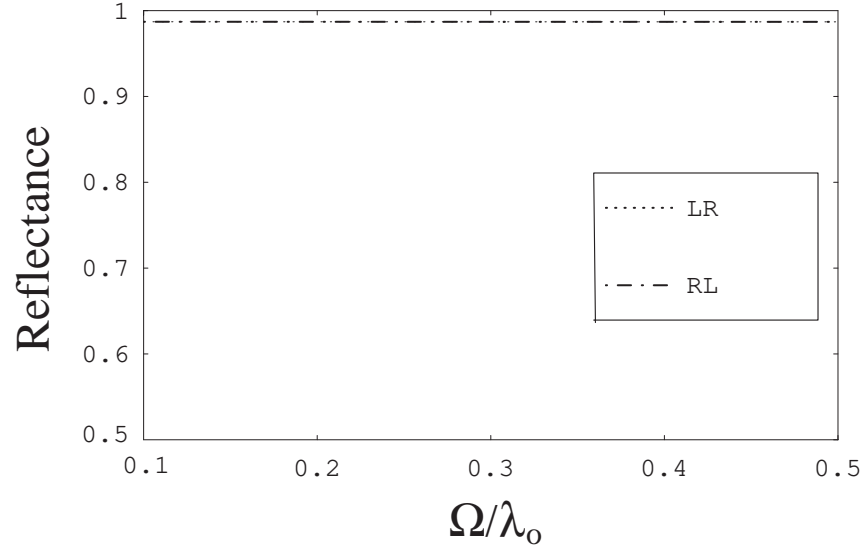


Figure 2: Computed values of the cross-polarized reflectances as functions of Ω/λ_0 , when $h = 1$, $\epsilon_c = 3(-1+0.01i)$ and $\tilde{\epsilon}_d = 3.3(-1+0.02i)$. Note that $R_{RL} \simeq R_{LR}$; while $R_{RR} \simeq 0$ and $R_{LL} \simeq 0$ cannot be discerned at the scale of the graph and are therefore not shown.